Manuscript for *Revista Mexicana de Astronomía y Astrofísica* (2009)

CONSTRAINING COSMOLOGICAL INFLATION

J. Alberto Vázquez, [1,3]

Draft version: November 30, 2015

RESUMEN

El objetivo de este artículo es ofrecer una introducción cualitativa a la teoría de la Inflación Cosmólogica y su relación con las observaciones cosmológicas actuales. Inflación resuelve algunos de los problemas fundamentales que desafían al modelo estándar de la cosmología (Big Bang), por ejemplo, el problema de la Planicidad, Horizonte y la inexistencia de Monopolos, y además de resolver estos problemas, explica el origen de la estructura a gran escala del Universo, como son las galaxias. Se describen las características generales de esta solución llevada a cabo por un campo escalar. Por último, con el uso de recientes (y futuros) estudios, se presentan constricciones de los parámetros inflacionarios $(n_{\rm s}, r)$ que nos permitirán realizar la conexión entre la teoría y las observaciones cosmológicas. De ésta manera, con los últimos resultados observacionales, es posible elegir o al menos limitar el modelo inflacionario correcto, parametrizado por el potencial de campo escalar $V(\phi)$.

ABSTRACT

The aim of this paper is to provide a qualitative introduction to the Inflationary theory and its relation with current cosmological observations. Inflation solves some of the fundamental problems which challenge the Standard Big Bang cosmology i.e. Flatness, Horizon and Monopole problem, and additionally explains the initial conditions for the Large-Scale Structure observed in the Universe, such as galaxies. We describe the general properties of this solution carried out by a single scalar field. Finally, with the use of current and future surveys, we show constraints on the Inflationary parameters $(n_{\rm s}, r)$ which allow us to make the connection between the theoretical and observational cosmology. In this way, with the latest observational results, it is possible to choose or at least to constrain the right Inflationary model, parameterised by the scalar field potential $V(\phi)$.

Key Words: cosmology: cosmological parameters — cosmology: observations — cosmology: inflation

1. INTRODUCTION

Nowadays, the Standard Big Bang (SBB) cosmology is the most accepted model describing the central features of the observed Universe. This model has been successfully proved on cosmological levels, for instance, numerical simulations on the structure formation of galaxies, galaxy clusters and so on

[1]Kavli Institute for Cosmology / Cavendish Laboratory, Cambridge, UK.
[3]Instituto Avanzado de Cosmología (IAC), http://www.iac.edu.mx/

are in good agreement with astronomical observations (Tegmark et al. 2001; Springel et al. 2005). The SBB model also predicts the fluctuations on the temperature observed in the Cosmic Microwave Background radiation (CMB) with high degree of accuracy: inhomogeneities of about one part in one hundred thousand (Komatsu et al. 2011). These two predictions, amongst many others, are the great success of the SBB cosmology. Nevertheless, when we look at cosmological observations, there might seem to exist certain inconsistencies or unexplained features in contrast with expected by the theory. Some of these unsatisfactory aspects led to the emergence of the Inflationary model (Guth 1981; Linde 1982, 1983; Albrecht & Steinhardt 1982).

In this work, we briefly present some of the relevant shortcomings the standard cosmology is dealing with and a short review is carried out about the scalar fields as promising solution. Moreover, it is shown how an inflationary single-field model can be completely described by only specifying its potential form $V(\phi)$. Based on the slow-roll approximation, it is found that the observational parameters which allow us to make the connexion with experiments are given by: the amplitude of density perturbation δ_H, the scalar spectral index $n_{\rm s}$ and the tensor-to-scalar ratio r. Finally, the theoretical predictions for different scalar field potentials are shown and compared with current observational data on the phase-space parameter $n_{\rm s} - r$, thus, constraining the number of candidates and making predictions on the shape of $V(\phi)$.

2. PROBLEMS IN THE SBB MODEL

Before starting with the theoretical description, let us consider some assumptions on which the SBB model is built (Coles & Lucchin 1995):

1) The physical laws at the present time can be extrapolated further back in time and also be considered as valid in the early Universe. In this context, gravity is described by the theory of General Relativity without a cosmological constant (Λ) up to the Plank era.

2) The cosmological principle holds: "There do not exist preferred places in the Universe". This is telling us that the properties of the Universe at large-scale must be the homogeneity and isotropy, both of them encoded on the Friedmann-Robertson-Walker (FRW) metric

$$ds^2 = -dt^2 + a^2(t)\left[\frac{dr^2}{1-kr^2} + r^2(d\theta^2 + sin^2\theta\, d\phi^2)\right], \tag{1}$$

where (t, r, θ, ϕ) describe the time-polar coordinates; the spatial curvature is given by the constant k and the scale-factor $a(t)$ represents the physical size of the Universe.

3) The anisotropic Universe is well described by a linear expansion of the metric about the FRW background:

$$g_{\mu\nu}(\mathbf{x}, t) = g^{FRW}_{\mu\nu}(\mathbf{x}, t) + h_{\mu\nu}(\mathbf{x}, t). \tag{2}$$

To avoid long calculations and make this article accessible to young scientists, many technical details have been omitted or simplified; we encourage the

reader to check out the vast amount of literature about the Inflationary theory (Liddle & Lyth 2000; Liddle 1999; Kolb & Turner 1994; Dodelson 2003; Linde 1990).

To describe the general properties of the Universe, we assume its dynamics is governed by a source treated as a perfect fluid with pressure $p(t)$ and density $\rho(t)$. Both quantities may often be related via an equation of state $p = p(\rho)$. Some of the well studied cases are

$$\begin{aligned} p &= \frac{\rho}{3} && \text{radiation,} \\ p &= 0 && \text{dust,} \\ p &= -\rho && \Lambda. \end{aligned} \tag{3}$$

The Einstein equations for these kind of constituents, neglecting the cosmological constant Λ contribution, are given by:
The **Friedmann equation**

$$H^2 \equiv \frac{8\pi}{3m_{Pl}^2}\rho - \frac{k}{a^2}, \tag{4}$$

and the **acceleration equation**

$$\frac{\ddot{a}}{a} = -\frac{4\pi}{3m_{Pl}^2}(\rho + 3p). \tag{5}$$

The energy conservation for the fluids is described by the **fluid equation**

$$\dot{\rho} + 3H(\rho + p) = 0, \tag{6}$$

where overdots mean time derivative and $H \equiv \dot{a}/a$ defines the *Hubble parameter*. Hereafter we employ natural units $c = \hbar = 1$; the Planck mass m_{Pl} is related with the gravitational constant G through $G \equiv m_{Pl}^{-2}$.

We notice, from (4), that for a particular Hubble parameter there exists a particular density for which the universe is spatially flat ($k = 0$). This is known as the *critical density* ρ_c and is given by

$$\rho_c(t) \;=\; \frac{3m_{Pl}^2\, H^2}{8\pi}, \tag{7}$$

where ρ_c is a function of time due to the presence of H. In particular, its present value is denoted as $\rho_{c,0} = 1.88\, h^2 \times 10^{-26}$ kg m^{-3}, or in terms of more convenient units taking into account large scales in the Universe, $\rho_{c,0} = 2.78\, h^{-1} \times 10^{11} M_\odot/(h^{-1}\mathrm{Mpc})^3$; with the solar mass denoted by $M_\odot = 1.988 \times 10^{33}$g and h parameterises the present value of the Hubble parameter as

$$H_0 = 100h\,\mathrm{km\,s^{-1}Mpc^{-1}} = \frac{h}{3000}\mathrm{Mpc}^{-1}. \tag{8}$$

The latest value for the Hubble parameter obtained by the *Hubble Space Telescope* is quoted to be (Riess 2009)

$$H_0 = 74.2 \pm 3.6\,\mathrm{kms}^{-1}\mathrm{Mpc}^{-1}. \tag{9}$$

Usually, it is more useful to measure the energy density as a fraction of the critical density, defining the *density parameter* $\Omega_i = \rho_i/\rho_c$. The label i represents different constituents of the Universe, such as radiation or matter. Then, the Friedmann equation (4) can then be written in such a way to directly relate the density parameter and the curvature of the Universe as

$$\Omega - 1 = \frac{k}{a^2 H^2}. \tag{10}$$

Thus, the correspondence between the matter content Ω and the space-time curvature for different k values is:

- Open Universe : $0 < \Omega < 1 : \; k < 0 : \; \rho < \rho_c$.
- Flat Universe : $\Omega = 1 : \; k = 0 : \; \rho = \rho_c$.
- Closed Universe: $\Omega > 1 : \; k > 0 : \; \rho > \rho_c$.

Current cosmological observations, based on the standard model, suggest the present value of Ω is (Komatsu et al. 2011)

$$\Omega_0 = 1.00 \pm 0.002, \tag{11}$$

that is, the present Universe is very nearly flat.

Shortcomings

Flatness problem

We notice that an special case of equation (10) is $\Omega = 1$. If at the beginning the Universe was perfectly flat, then it remains so for all time. Nevertheless, a flat geometry is an unstable critical situation, that is, even a tiny deviation from it, Ω would evolve quite different and very quickly the Universe would become more curved. This can be seen as a consequence due to aH is a decreasing function of time during radiation or matter domination epoch. We observe it from (10):

$$\begin{aligned} |\,\Omega - 1\,| &\propto t && \text{radiation domination,} \\ |\,\Omega - 1\,| &\propto t^{2/3} && \text{dust domination.} \end{aligned}$$

Since the present age of the Universe is estimated to be $t_0 \simeq 10^{17}\,\mathrm{sec}$ (Larson et al. 2011), from the above equation we can deduce the required value of $|\,\Omega - 1\,|$ at different early-times in order to obtain the correct value of spatial-geometry at present time. For instance, let us consider some particular epochs in a nearly flat universe,

- Decoupling ($t \simeq 10^{13}\,\mathrm{sec}$), we need $\mid \Omega - 1 \mid \leq 10^{-3}$.
- Nucleosynthesis ($t \simeq 1\,\mathrm{sec}$), we need $\mid \Omega - 1 \mid \leq 10^{-16}$.
- Planck epoch ($t \simeq 10^{-43}\,\mathrm{sec}$), we need $\mid \Omega - 1 \mid \leq 10^{-64}$.

Because there is no reason to prefer a Universe with critical density, hence $\mid \Omega - 1 \mid$ should not necessarily be exactly zero. Consequently, at early times $\mid \Omega - 1 \mid$ have to be fine-tuned extremely close to zero in order to reach its actual observed value.

Horizon problem

The horizon problem is one of the most important problems in the Big Bang model, it refers to the communication between different regions of the Universe. Bearing in mind the *Anthropic Cosmological Principle* holds (Barrow & Tipler 1986; Coles & Lucchin 1995), which is intimately connected with the existence of the Big Bang, the age of the Universe is a finite quantity and hence even light should have only travelled a finite distance by any given time.

According the standard cosmology, photons decoupled from the rest of the components at temperatures about $T_{dec} \approx 0.3\,eV$ at redshift $z_{dec} \approx 1100$, from this time on photons free-streamed and travelled basically uninterrupted until reach us, giving rise to the region known as the Observable Universe. This spherical surface at which decoupling process occurred is called *surface of last scattering*. The primordial photons are responsible for the CMB observed today, then looking at the fluctuations is analogous of taking a picture of the universe at this time ($t_{dec} \approx 380,000$ yrs old), see Figure 1.

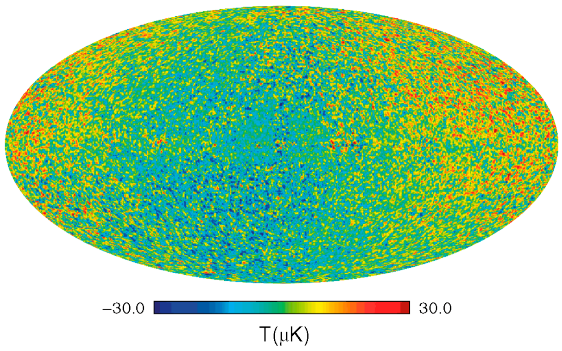

Fig. 1. Temperature fluctuations observed in the CMB using WMAP seven year data (Gold et al. 2011).

Figure 1 shows light seen in all directions of the sky, these photons randomly distributed have nearly the same temperature $T_0 = 2.725$ K plus small fluctuations (about one part in one hundred thousand). As we have already noted, being at the same temperature is a property of thermal equilibrium, thus observations are easily explained if different regions of the sky have been

able to interact and moved towards thermal equilibrium. In other words, the isotropy observed in the CMB might imply that the radiation was homogeneous and isotropic in regions located on the last scattering surface.

Oddly, the comoving horizon over which causal interactions occurred before photons decoupled was significantly smaller than the comoving distance that radiation travelled after decoupling. This means that photons coming from separated sky regions by more than the horizon scale at last scattering, typically about 2°, would not have been able to interact and established thermal equilibrium before decoupling. A simple calculation displays that at decoupling time the comoving horizon was 90 h^{-1} Mpc and would be stretched up to 2998 h^{-1} Mpc at present time. Then, the microwave background should have consisted of about 10^4 causally disconnected regions. Therefore, the Big Bang model by itself does not offer an explanation on why temperatures seen in opposite sides of the sky are so accurately the same; the homogeneity must have been part of the initial conditions.

On the other hand, the microwave background is not perfectly isotropic, but instead exhibits small fluctuations as detected by, initially, the Cosmic Background Explorer satellite (COBE) (Smooth et al. 1992) and now, with improved measurements by the Wilkinson Microwave Anisotropy Probe (WMAP) (Hinshaw et al. 2009; Larson et al. 2011). These tiny irregularities are thought to be the 'seeds' that grew up until become the structure nowadays observed in the Universe.

Monopole problem

Following the line to find out the simplest theory to describe entirely the laws of the Universe, several models in particle physics were suggested to unified three of the four forces presented in the Standard Model of Particle Physics (SM): strong force, described by the group $SU(3)$, weak and electromagnetic force, with associated group $SU(2) \otimes U(1)$. These classes of theories are called *Grand Unified Theories (GUT)* (Georgi & Glashow 1974). An important point to mention in favour of GUT, is that they are the only theories which predict the equality electron-proton charge magnitude. Also, there are good reasons to believe that the origin of *baryon asymmetry* might have been generated by GUTs (Kolb & Turner 1983).

Basically, these kind of theories assert that in the early Universe ($t \sim 10^{-43}$ sec), at highly extreme temperatures ($T_{GUT} \sim 10^{32}$ K), existed a unified or *symmetric phase* described by a group G. As the Universe temperature dropped off, it went through many different phase transitions until reach the matter particles such as electrons, protons, neutrons, photons. When a phase transition happens, its symmetry is broken, thus the symmetry group changes by itself. For instance:

- GUT transition:

$$G \to SU(3) \otimes SU(2) \otimes U(1).$$

- Electroweak transition:

$$SU(3) \otimes SU(2) \otimes U(1) \to SU(3) \otimes U(1).$$

The phase transitions have plenty of implications, one of the most important is the *topological defects* production, that depends on the type of symmetry breaking and the spatial dimension (Vilenkin & Shellard 2000), some of them are:

- Monopoles (zero dimensional).
- Strings (one dimensional).
- Domain Walls (two dimensional).
- Textures (three dimensional).

Therefore, monopoles are expected to emerge as a consequence of unification models. Besides that, from particle physics models, monopoles would have a mass of 10^6 orders the proton mass. Hence, based on their non-relativitic character, a crude calculation predicts an extremely high abundance at present time (Coles & Lucchin 1995)

$$\Omega_M \simeq 10^{16}.$$

According to this prediction, the Universe would be dominated by magnetic monopoles. However, in contrast with current observations, no one has found anyone (Ambrosio 2002).

3. COSMOLOGICAL INFLATION

The inflationary model offers the most elegant way so far proposed to solve the problems aforementioned and therefore to understand why the universe is so remarkably in agreement with the standard cosmology. It does not replace the Big Bang model, but rather it is considered as an 'auxiliary patch' which occurred at the earliest stages without disturbing any of its successes.

Inflation is defined as the epoch in the evolution of the Universe in which the scale factor is quickly accelerated in just a fraction of a second:

$$\text{INFLATION} \iff \ddot{a} > 0 \tag{12}$$

$$\iff \frac{d}{dt}\left(\frac{1}{aH}\right) < 0. \tag{13}$$

The last term corresponds to the comoving Hubble length $1/(aH)$ which is interpreted as the observable Universe becoming smaller during inflation. This process allows our observable region to lie within a region that was inside the Hubble radius at the beginning of inflation, in Liddle (1999) words "is something similar to zooming in on a small region of the initial universe", see Figure 2.

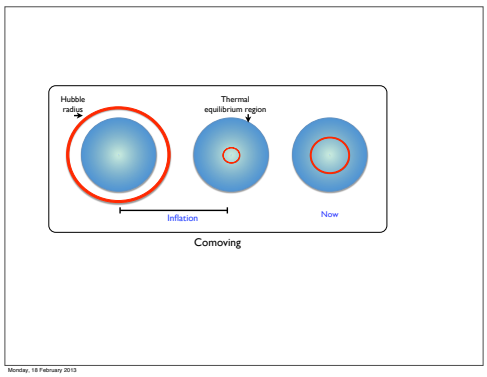

Fig. 2. Schematic behaviour of the comoving Hubble radius during the Inflationary period

From the acceleration equation (5) we can write the condition for inflation in terms of the material required to drive the expansion

$$\ddot{a} > 0 \Longleftrightarrow (\rho + 3p) < 0. \tag{14}$$

Because in standard physics it is always postulated ρ as positive, to satisfy the acceleration condition it is necessary for the overall pressure to have

$$\text{INFLATION} \iff p < -\rho/3. \tag{15}$$

Nonetheless, neither a radiation nor a matter dominated epoch satisfies such condition. Let us postpone for a while the problem of finding a 'candidate' which may satisfy this inflationary condition.

3.1. *Solution of the Big Bang Problems*

Flatness problem

If this brief period of accelerated expansion occurred, then it is possible that the aforementioned problems of the Big Bang could be solved. A typical solution is a universe possessing a cosmological constant Λ, which can be interpreted as a perfect fluid with equation of state $p = -\rho$. Having this condition, since H is constant, we observe from the Friedmann equation (4) that the universe is exponentially expanded:

$$a(t) \propto \exp(Ht), \tag{16}$$

then, the condition (13) is naturally fulfilled. This epoch is called *de Sitter stage*. However, postulating a cosmological constant might create more problems than solve by itself (Carroll 2001).

Let us look what happens when a general solution is considered. If somehow there was an accelerated expansion, $1/(aH)$ tends to be smaller on time and hence, by the expression (10), Ω is driven towards the unity rather than away from it. Then, we may ask ourselves by how much should $1/(aH)$ decrease. If the inflationary period started at time $t = t_i$ and ended up approximately at the beginning of the radiation dominated era ($t = t_f$), then

$$\mid \Omega - 1 \mid_{t=t_f} \sim 10^{-60},$$

and

$$\frac{\mid \Omega - 1 \mid_{t=t_f}}{\mid \Omega - 1 \mid_{t=t_i}} = \left(\frac{a_i}{a_f}\right)^2 \equiv e^{-2N}. \tag{17}$$

So, the required condition to reproduce the value of Ω_0 today is that inflation lasted for at least $N \equiv \ln a \gtrsim 60$, then Ω will be extraordinarily close to one that we still observe it today. In this sense, inflation magnifies the curvature radius of the universe, so locally the universe seems to be flat with a great precision.

Horizon problem

As we have already seen, during inflation the universe expands drastically and there is a reduction in the comoving Hubble length. This allowed a tiny region located inside the Hubble radius to evolve and constitute our present observable Universe. Fluctuations were hence stretched outside of the horizon during inflation and re-entered the horizon in the late Universe, see Figure 2. Scales that were outside the horizon at CMB decoupling were in fact inside the horizon before inflation. The region of space corresponding to the observable universe therefore was in thermal equilibrium before inflation and the uniformity of the CMB is essentially explained.

Monopole problem

The monopole problem was initially the motivation to develop the Inflationary cosmology (Guth 1997). During the inflationary epoch, the Universe led to a dramatic expansion over which the density of the unwanted particles were diluted away. Generating enough expansion, the dilution made sure the particles stayed completely out of our observable Universe making pretty difficult to localise a single monopole.

4. SINGLE-FIELD INFLATION

There currently exists a broad diversity of models that have been proposed for inflation (Liddle & Lyth 2000; Olive 1990; Lyth & Riotto 1999). In this section we present the scalar fields as good candidates to drive inflation and explain how relate theoretical predictions to observable quantities. Here, we limit ourselves to models based on general gravity, i.e. derived from the Einstein-Hilbert action, and single-field models described by a slow-roll scalar field ϕ.

Inflation relies on the existence of an early epoch in the universe dominated by a very different form of energy; remember the requirement of the unusual property of a negative pressure. Such condition can be satisfied by a simple scalar field (spin-0 particle). The scalar field which drives the Universe to an inflationary epoch is often termed as the *inflaton field*.

Let us consider a scalar field minimally coupled to gravity, with an arbitrary potential $V(\phi)$ and Lagrangian density $\mathcal{L}$ specified by

$$S = \int d^4x \sqrt{-g}\, \mathcal{L} = \int d^4x \sqrt{-g} \left[\frac{1}{2} \partial_\mu \phi \partial^\mu \phi - V(\phi) \right]. \tag{18}$$

The energy-momentum tensor corresponding to this scalar field Lagrangian is given by

$$T_{\mu\nu} = \partial_\mu \phi \partial_\nu \phi - g_{\mu\nu}\, \mathcal{L}. \tag{19}$$

In the same way as the perfect fluid treatment, the energy density ρ_ϕ and pressure density p_ϕ in FRW metric are found to be

$$T_{00} = \rho_\phi = \frac{1}{2}\dot{\phi}^2 + V(\phi) + \frac{(\nabla\phi)^2}{2a^2}, \tag{20}$$

$$T_{ii} = p_\phi = \frac{1}{2}\dot{\phi}^2 - V(\phi) - \frac{(\nabla\phi)^2}{6a^2}, \tag{21}$$

with equation of state corresponding to

$$w = \frac{P}{\rho} = \frac{\frac{1}{2}\dot{\phi}^2 - V(\phi)}{\frac{1}{2}\dot{\phi}^2 + V(\phi)}. \tag{22}$$

We can now split the inflaton field as

$$\phi(\mathbf{x}, t) = \phi_0(t) + \delta\phi(\mathbf{x}, t), \tag{23}$$

where ϕ_0 is considered a classical field, that is, the mean value of the inflaton field on the homogeneous and isotropic state, whereas $\delta\phi(\mathbf{x}, t)$ describes the quantum fluctuations around ϕ_0.
The evolution equation for the background field ϕ_0 is given by

$$\ddot{\phi_0} + 3H\dot{\phi_0} = -V'(\phi_0), \tag{24}$$

and moreover, the Friedmann equation (4) with negligible curvature becomes

$$H^2 = \frac{8\pi}{3m_{Pl}^2}\left[\frac{1}{2}\dot{\phi}_0^2 + V(\phi_0)\right], \tag{25}$$

where we have used primes as derivatives with respect to the scalar field ϕ_0.

From the structure of the effective energy density and pressure, the acceleration equation (5) becomes,

$$\frac{\ddot{a}}{a} = -\frac{8\pi}{m_{Pl}^2}\left(\dot{\phi}_0^2 - V(\phi_0)\right). \tag{26}$$

Therefore, the inflationary condition to be satisfied is $\dot{\phi}_0^2 < V(\phi_0)$, and it is easily fulfilled with a suitably flat potential. Now on we will omit the subscript '0' by convenience.

4.1. *Slow-roll approximation*

As we have noted, a period of accelerated expansion can be created by the cosmological constant (Λ) and hence solve the problems aforementioned. After a brief period of time, inflation must end up and its energy being converted into conventional matter/radiation, this process is called *reheating*. In a Universe dominated by a cosmological constant the reheating process is seen as Λ decaying into conventional particles. However, claiming that Λ is able to decay is still a naive way to face the problem. On the other hand, scalar fields have the property to behave like a *dynamical cosmological constant*. Based on this approach, it is useful to propose a scalar field model starting with a nearly flat potential, i.e. initially satisfies the condition $\dot{\phi}^2 \ll V(\phi)$. In this case the scalar field is slowly rolling down its potential, by obvious reasons, such approximation is called *slow-roll* (Liddle & Lyth 1992; Liddle et al. 1994). Based on this approach, $\ddot{\phi}$ is negligible because the Universe is dominated by the cosmological expansion. The equations of motion (24) and (25), for slow-roll inflation, then become

$$3H\dot{\phi} \simeq -V'(\phi), \tag{27}$$

$$H^2 \simeq \frac{8\pi}{3m_{Pl}^2}V(\phi). \tag{28}$$

It is easily verifiable that the slow-roll approximation requires the slope and curvature of the potential to be small: $V', V'' \ll V$.

The Inflationary process can be summarised as an accelerated Universe which takes place when the kinetic part of the inflaton field is subdominant over the potential field $V(\phi)$ term. Then, when both quantities become comparable the Inflationary period ends up given rise finally to the reheating process, see Fig. 3.

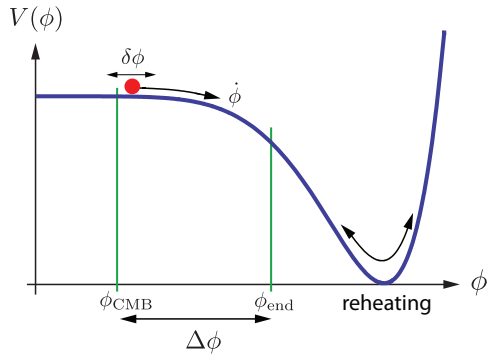

Fig. 3. Schematic Inflationary process (Baumann & Peiris 2009).

It is now useful to introduce the potential slow-roll parameters $\epsilon_{\rm v}$ and $\eta_{\rm v}$ in the following way (Liddle & Lyth 1992)

$$\epsilon_{\rm v}(\phi) \equiv \frac{m_{Pl}^2}{16\pi}\left(\frac{V'(\phi)}{V(\phi)}\right)^2, \tag{29}$$

$$\eta_{\rm v}(\phi) \equiv \frac{m_{Pl}^2}{8\pi}\frac{V''(\phi)}{V(\phi)}. \tag{30}$$

Equations (27) and (28) are in agreement with the slow-roll approximation when the following conditions hold

$$\epsilon_{\rm v}(\phi) \ll 1, \quad |\,\eta_{\rm v}(\phi)\,| \ll 1.$$

These conditions are sufficient but not necessary, because the validity of the slow-roll approximations was a requirement in its derivation. The physical meaning of $\epsilon_{\rm v}(\phi)$ can be explicitly seen by expressing equation (12) in terms of ϕ, then, the inflationary condition is equivalent to

$$\frac{\ddot{a}}{a} > 0 \implies \epsilon_{\rm v}(\phi) < 1. \tag{31}$$

Hence, inflation ends up when the value $\epsilon_{\rm v}(\phi_{end}) = 1$ is approached.

Within these approximations, it is straightforward to find out the scale factor a between the beginning and the end of inflation. Because the size of the expansion is an enormous quantity, it is useful to compute it in terms of the e-fold number N defined by

$$N \equiv \ln\frac{a(t_{end})}{a(t)} = \int_t^{t_e} H\,dt \simeq \frac{8\pi}{m_{Pl}^2}\int_{\phi_e}^{\phi}\frac{V}{V'}d\phi. \tag{32}$$

To give an estimate of the number of e-folds N, let us consider the evolution of the Universe can be split into different epochs:

- Inflationary era: horizon crossing ($k = aH$) $\rightarrow$ end of inflation a_{end}.

- Radiation era: reheating $\rightarrow$ matter-radiation equality a_{eq}.
- Matter era: $a_{eq} \rightarrow$ present a_0.

Assuming the transition between one era to another is instantaneous, then $N(k) = \ln(a_k/a_0)$ can be easily computed with:

$$\frac{k}{a_0 H_0} = \frac{a_k H_k}{a_0 H_0} = \frac{a_k}{a_{end}} \frac{a_{end}}{a_{reh}} \frac{a_{reh}}{a_{eq}} \frac{a_{eq}}{a_0} \frac{H_k}{H_0}.$$

Then, one has (Liddle & Lyth 2000)

$$N(k) = 62 - \ln \frac{k}{a_0 H_0} - \ln \frac{10^{16} GeV}{V_k^{1/4}} + \ln \frac{V_k^{1/4}}{V_{end}} - \frac{1}{3} \ln \frac{V_{end}^{1/4}}{\rho_{reh}^{1/4}}.$$

The last three terms are small quantities related with energy scales during the inflationary process and usually can be ignored. The precise value for the second quantity depends on the model as well as the COBE normalisation, however it does not present any significant change to the total amount of e-folds. Thus, the value for total e-foldings is ranged from 50-70 (Lyth & Riotto 1999).

As we noted, the parameters to describe inflation can be presented as functions of the scalar field potential. That is, specifying an inflationary model with a single scalar field is just selecting an inflationary potential $V(\phi)$. In order to exemplify our point, let us consider the following example.

The potential which describes a massive scalar field is given by:

$$V(\phi) = \frac{1}{2} m^2 \phi^2. \tag{33}$$

Considering the slow-roll approximation, equations (24) and (25) become:

$$\begin{aligned} 3H\dot{\phi} &= -m^2 \phi, \\ H^2 &= \frac{4\pi m^2 \phi^2}{3 m_{pl}^2}. \end{aligned} \tag{34}$$

Thus, the dynamics of this type of model is described by

$$\begin{aligned} \phi(t) &= \phi_i - \frac{m m_{pl}}{\sqrt{12\pi}}, \\ a(t) &= a_i \exp\left[\sqrt{\frac{4\pi}{3}} \frac{m}{m_{pl}} \left(\phi_i t - \frac{m m_{pl}}{\sqrt{48\pi}} t^2 \right) \right], \end{aligned} \tag{35}$$

where ϕ_i and a_i represent the initial conditions at a given initial time $t = t_i$. The slow-roll parameters for this particular potential are computed from equations (29) and (30)

$$\epsilon_{\rm v} = \eta_{\rm v} = \frac{m_{pl}^2}{4\pi} \frac{1}{\phi^2}, \tag{36}$$

that is, an inflationary epoch takes place whilst the condition $|\phi| > m_{pl}/\sqrt{4\pi}$ is satisfied, and the total amount lapse during this accelerated period is encoded on the e-folds number

$$N_{tot} = \frac{2\pi}{m_{pl}^2}\left[\phi_i^2 - \phi_e^2\right]. \tag{37}$$

The steps shown before might, in principle, apply to any inflationary single-field model. That is, the general information we need to characterised cosmological inflation is specified by only its potential.

4.2. *Cosmological Perturbations*

Inflationary models have the merit that they do not only explain the homogeneity of the universe on large-scales, but also provide a theory for explaining the observed level of *anisotropy*. During the inflationary period, quantum fluctuations of the field were driven to scales much larger than the Hubble horizon. Then in this process, the fluctuations were frozen and turned into metric perturbations (Mukhanov & Chibisov 1997). Metric perturbations created during inflation can be described in terms of two types of perturbations. The *scalar, or curvature,* perturbations are coupled with matter in the universe and form the initial "seeds" of structure formation. On the other hand, although the *tensor perturbations* do not couple to matter, they are associated to the generation of gravitational waves. As we shall see, scalar and tensor perturbations are seen as the important components to the CMB anisotropy (Hu & Dodelson 2002).

In the same way we have introduced the density parameter for large scales, on small scales we employ the *density contrast* defined by $\delta \equiv \delta\rho/\rho$. We now on assume the density contrast for different species in the Universe satisfies the *adiabatic conditions*

$$\frac{1}{3}\delta_{\mathbf{k}b} = \frac{1}{3}\delta_{\mathbf{k}c} = \frac{1}{4}\delta_{\mathbf{k}\gamma}\left(= \frac{1}{4}\delta_{\mathbf{k}}\right). \tag{38}$$

The most general perturbation on the density is described by a linear combination between adiabatic perturbation as well as *isocurvature perturbation*, which the latter one plays and important role when more than one scalar field is considered (Liddle & Lyth 2000).

We introduce the *primordial curvature perturbation* $\mathcal{R}_k(t)$, which has the property to be constant within few Hubble times after the horizon exit given by $k = aH$. This constant value is called the *primordial value* and is related with the scalar field perturbation $\delta\phi$ by

$$\mathcal{R}_k = -\left[\frac{H}{\dot{\phi}}\ \delta\phi_k\right]_{k=aH}. \tag{39}$$

Then, the primordial curvature power spectrum $\mathcal{P}_{\mathcal{R}}(k)$ is computed from

$$\mathcal{P}_{\mathcal{R}}(k) = \left[\left(\frac{H}{\dot{\phi}}\right)^2 \mathcal{P}_{\phi}(k)\right]_{k=aH}. \tag{40}$$

When the perturbation part of $\phi(\mathbf{x},t)$ in (23) is considered, the equation of motion for $\delta\phi$ is described by

$$(\delta\phi_k)^{\cdot\cdot} + 3H(\delta\phi_k)^{\cdot} + \left(\frac{k}{a}\right)^2 \delta\phi_k = 0, \tag{41}$$

where we have assumed $\delta\phi$ is linear. This basically means that perturbations generated by vacuum fluctuations have uncorrelated Fourier modes, the signature of *Gaussian perturbations*. After scalar field quantisation, the spectrum is given by

$$\mathcal{P}_\phi(k) = \left(\frac{H}{2\pi}\right)^2_{k=aH}. \tag{42}$$

Finally, from (42) and (40) the spectrum of the curvature perturbation is

$$\mathcal{P}_\mathcal{R}(k) = \left[\left(\frac{H}{\dot\phi}\right)\left(\frac{H}{2\pi}\right)\right]^2_{k=aH}. \tag{43}$$

On the other hand, the creation of gravitational waves corresponds to the tensor part of metric perturbation $h_{\mu\nu}$ in (2). In Fourier space, tensor perturbation h_{ij} can be expressed as the superposition of two polarisation modes

$$h_{ij} = h_+ e^+_{ij} + h_\times e^\times_{ij}, \tag{44}$$

where $+$, $\times$ represent the longitudinal and transverse modes. From Einstein equations it is found that each amplitude h_+ and $h_\times$ behaves as a free scalar field in the sense that

$$\psi_{+,\times} \equiv \frac{m_{Pl}}{\sqrt{8}}\, h_{+,\times}. \tag{45}$$

Therefore, each $h_{+,\times}$ has a spectrum $\mathcal{P}_T$ given by

$$\mathcal{P}_T(k) = \frac{8}{m^2_{Pl}}\left(\frac{H}{2\pi}\right)^2_{k=aH}. \tag{46}$$

The canonical normalisation of the field $\psi_{+,\times}$ was chosen such that, the *ratio of tensor-to-scalar* spectra is

$$r \equiv \frac{\mathcal{P}_T}{\mathcal{P}_\mathcal{R}} = 4\pi\epsilon. \tag{47}$$

During the horizon exit epoch $k = aH$, H and $\dot\phi$ have tiny variations during few Hubble times. In this case, the scalar and tensor spectra are nearly scale independent and therefore well approximated by power laws

$$\begin{aligned} \mathcal{P}_\mathcal{R}(k) &= \mathcal{P}_\mathcal{R}(k_0)\left(\frac{k}{k_0}\right)^{n_\mathrm{s}-1}, \\ \mathcal{P}_T(k) &= \mathcal{P}_T(k_0)\left(\frac{k}{k_0}\right)^{n_T}. \end{aligned} \tag{48}$$

where the spectral indices are defined as (Lidsey 1997)

$$n_{\rm s} - 1 \equiv \frac{d \ln \mathcal{P}_{\mathcal{R}}(k)}{d \ln k}, \qquad n_T \equiv \frac{d \ln \mathcal{P}_T(k)}{d \ln k}. \tag{49}$$

A scale-invariant spectrum, called Harrison-Zel'dovich (HZ), has constant variance on all length scales and it is characterised by $n_{\rm s} = 1$. Small deviations from scale-invariance are also considered as a typical signature of the inflationary models, then the spectral indices $n_{\rm s}$ and n_T can be expressed in terms of the slow-roll parameters $\epsilon_{\rm v}$ and $\eta_{\rm v}$, to lowest order, as:

$$\begin{aligned} n_{\rm s} - 1 &\simeq -6\ \epsilon_{\rm v}(\phi) + 2\ \eta_{\rm v}(\phi), \\ n_T &\simeq -2\ \epsilon_{\rm v}(\phi). \end{aligned} \tag{50}$$

The parameters are *not* completely independent each other, but the tensor spectral index is proportional to the tensor-to-scalar ratio $r = -2\pi n_T$. This expression is considered as the *consistency relation* for slow-roll inflation. Hence, any inflationary model, to the lowest order in slow-roll, can be described in terms of three independent parameters: the amplitude of density perturbations $\delta_H \equiv 2/5 P_{\mathcal{R}}^{1/2} \approx 2 \times 10^{-5}$, the scalar spectral index $n_{\rm s}$, and the tensor-to-scalar ratio r. In case we need a more accurate description we have to consider higher-order effects, and then include parameters for describing the running of scalar ($dn_{\rm s}/d\ln k$) and tensor ($dn_T/d\ln k$) index.

An important point to emphasised is that δ_H, r and $n_{\rm s}$ are *observable* parameters that nowadays are tested from several experiments. This allows us to compare theoretical predictions with observational data, for instance, those provided by the Cosmic Microwave Background radiation. In other words, future measurements of these parameters may probe or at least constrain the inflationary models and therefore the shape of the inflaton potential $V(\phi)$.

Let us back to the massive scalar field example in equation (33): Inflation ends up when the condition $\epsilon_{\rm v} = 1$ is achieved, so $\phi_{end} \simeq m_{pl}/\sqrt{4\pi}$. As we pointed out before, we are interested in models with an e-fold number of about $N_{tot} = 60$, that is

$$\phi_i = \phi_{60} \simeq \sqrt{\frac{30}{\pi}} m_{pl}. \tag{51}$$

Finally, the spectral index and the tensor-scalar ratio for this potential are

$$n_{\rm s} - 1 = -\frac{m_{pl}^2}{\pi \phi_{60}^2}, \qquad r = \frac{m_{pl}^2}{\phi_{60}^2}. \tag{52}$$

If the massive scalar field potential is the right inflationary model, current observations should favour the values $n_s \approx 0.97$ and $r \approx 0.1$.

5. INFLATIONARY MODELS

We have seen that an inflationary model is described by the specification of the potential form $V(\phi)$ relevant during inflation. Then, the comparison of inflationary model predictions to CMB observations reduces to the following basic steps (Kinney et al. 2006): (1) Given a scalar field potential $V(\phi)$, compute the slow roll parameters $\epsilon_{\rm v}(\phi)$ and $\eta_{\rm v}(\phi)$. (2) Find out ϕ_{end} by $\epsilon(\phi_{end}) = 1$. (3) From (32), compute the field ϕ_{60}. (4) Compute r and $n_{\rm s}$ as functions of ϕ, and finally evaluate them at $\phi = \phi_{60}$ which can be tested by CMB temperature anisotropy data.

Different types of models are classified by the relation among their slow-roll parameters ϵ and η, which can be reflected on different relations between r and $n_{\rm s}$. Hence, an appropriate parameter space to show the diversity of models is well described by the $n_{\rm s}$—r plane.

5.1. *Models*

Even if we restrict the analysis to a simple single-field, the number of inflationary models available is enormous (Liddle & Lyth 2000; Lyth & Riotto 1999; Linde 2005). Then, it is convenient to classify different kinds of scalar field potentials following (Kinney 2004).

The classification is based on the behaviour of the scalar field potential during inflation. The three basic types are shown in Figure 4. *Large field*, the field is initially displaced from an stable minimum and evolves towards it. *Small field*, the field evolves away from an unstable maximum. *Hybrid*, the field evolves towards a minimum with vacuum energy different to zero.

A general single field potential can be written in terms of a *height* Λ and a *width* μ as

$$V(\phi) = \Lambda^4 f\left(\frac{\phi}{\mu}\right). \tag{53}$$

Different models have different forms for the function f.

5.2. *Large-field models:* $-\epsilon < \eta \leq \epsilon$

Large field models perhaps posses the simplest type of monomial potentials. These kind of potentials represent the *chaotic* inflationary scenarios (Linde 1983). The distinctive of these models is that the shape of the effective potential is not very important in detail. That is, a region of the Universe where the scalar field is usually situated at $\phi \sim m_{\rm Pl}$ from the minimum of its potential will automatically lead to inflation, see Figure 5. Such models are described by $V''(\phi) > 0$ and $-\epsilon < \eta \leq \epsilon$.

A general set of large-field polynomial potentials can be written as

$$V(\phi) = \Lambda^4 \left(\frac{\phi}{\mu}\right)^p, \tag{54}$$

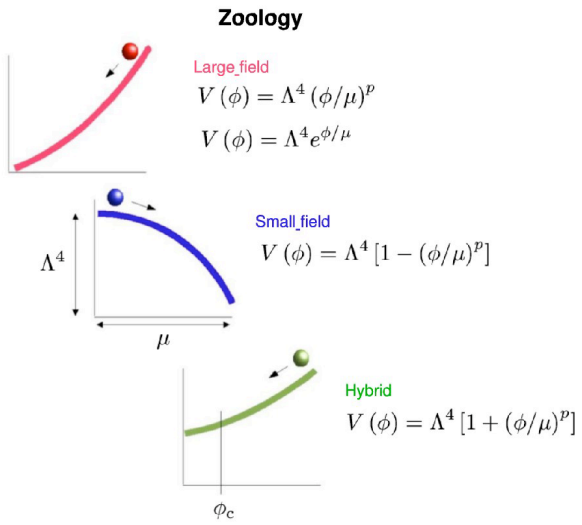

Fig. 4. Potential classification. From top to bottom: *large field, small field and hybrid potential* (Kinney 2004).

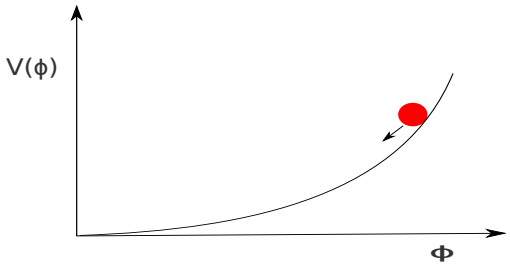

Fig. 5. Chaotic Inflationary potential.

where it is enough to choose the exponent $p > 1$ in order to specify a particular model. This model gives

$$\begin{aligned} n_s - 1 &= -\frac{4+2p}{4N+p}, \\ r &= \frac{4\pi p}{4N+p}. \end{aligned} \tag{55}$$

In this case, gravitational waves can be sufficiently big to eventually be observed ($r \gtrsim 0.1$).

From the quadratic potential of equation (33), we obtain

$$\epsilon \simeq 0.008, \quad \eta \simeq 0.008, \quad n_s \simeq 0.97, \quad r \simeq 0.1 \tag{56}$$

In the high power limit the $V \propto \phi^p$ predictions are the same as the exponential potential (La & Steinhardt 1999). Hence, a variant of this class of models is

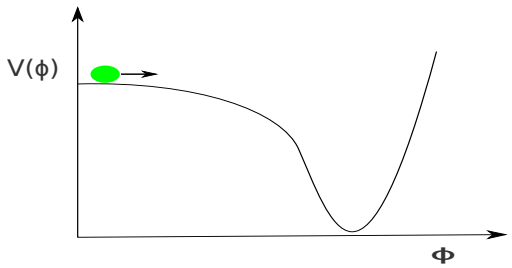

Fig. 6. New Inflationary potential.

$$V(\phi) = \Lambda^4 \exp(\phi/\mu). \tag{57}$$

This type of potential is a rare case presented in inflation, that is because its dynamics has an exact solution given by a power-law expansion. For this case the spectral index n_s is closely related to the tensor-to-scalar ratio r, as

$$\begin{aligned} n_s - 1 &= -\frac{m_{pl}^2}{8\pi\mu^2}, \\ r &= 2\pi(1 - n_s), \end{aligned} \tag{58}$$

as we observe, the slow-roll parameters are explicitly independent of the e-fold number N.

5.3. *Small-field models:* $\eta < -\epsilon$

Small field models are typically described by potentials which arise naturally from spontaneous symmetry breaking, these type of models are also known as *new inflation* (Albrecht & Steinhardt 1982; Linde 1983). In this case, inflation takes place when the field is situated in a false vacuum state, very close to the top of the hill and rolls down to a stable minimum, see Figure 6. These models are typically characterized by $V''(\phi) < 0$ and $\eta < -\epsilon$, usually ϵ (and hence the tensor amplitude) is closely zero.
Small field potentials, can be written in the generic form as

$$V(\phi) = \Lambda^4 [1 - (\phi/\mu)^p], \tag{59}$$

where the exponent p differs from model to model. $V(\phi)$ is usualy considered as the lowest-order in a Taylor expansion from a more general potential. In the simplest case of spontaneous symmetry breaking with no special symmetries, the dominant term is the mass term, $p = 2$, hence the model gives

$$\begin{aligned} n_s - 1 &\simeq -4\left(\frac{m_{\rm Pl}}{\mu}\right)^2, \\ r &= 2\pi(1 - n_s)\exp[-1 - N(1 - n_s)]. \end{aligned} \tag{60}$$

On the other hand, $p > 2$ has a very different behavior. The scalar spectral index is

$$n_{\rm s} - 1 = -\frac{2}{N}\left(\frac{p-1}{p-2}\right), \tag{61}$$

independent of $(m_{\rm Pl}/\mu)$. In addition, if it is considered $\mu < m_{\rm Pl}$ the values of r are restricted by

$$r < 2\pi \frac{p}{N\,(p-2)}\left[\frac{8\pi}{Np\,(p-2)}\right]^{p/(p-2)}. \tag{62}$$

5.4. *Hybrid models:* $0 < \epsilon < \eta$

The third class called **hybrid** frequently includes models which incorporate supersymmetry into inflation (Linde 1991; Copeland et al. 1994). In these models, the inflaton field ϕ evolves towards a minimum of its potential, however, the minimum has a vacuum energy $V(\phi_{\rm min}) = \Lambda^4$ which is different to zero. In such cases, inflation continues forever unless an auxiliary field ψ is added to interact with ϕ and ends inflation at some point $\phi = \phi_{\rm c}$. Such models are well described by $V''(\phi) > 0$ and $0 < \epsilon < \eta$.

The generic potential for hybrid inflation, in a similar way to large field and small field models are considered, is

$$V(\phi) = \Lambda^4\left[1 + (\phi/\mu)^p\right]. \tag{63}$$

For $(\phi_N/\mu) \gg 1$ the behaviour of the large-field models is recovered. Besides that, when $(\phi_N/\mu) \ll 1$, the dynamics is similar to small-field models, but now the field is evolving towards a dynamical fixed point rather than away from it. Because the presence of an auxiliary field, the number of e-folds is

$$N(\phi) \simeq \left(\frac{p+1}{p+2}\right)\left[\frac{1}{\eta(\phi_c)} - \frac{1}{\eta(\phi)}\right]. \tag{64}$$

For $\phi \gg \phi_c$, $N(\phi)$ approaches the value

$$N_{max} \equiv \left(\frac{p+1}{p+2}\right)\frac{1}{\eta(\phi_c)}, \tag{65}$$

and therefore, the spectral index is given by

$$n_{\rm s} - 1 \simeq 2\left(\frac{p+1}{p+2}\right)\frac{1}{N_{max} - N}.$$

As we can note, the power spectrum is *blue* ($n_{\rm s} > 1$) and besides that, the model presents a running of the spectral index

$$\frac{dn_{\rm s}}{d\ln k} = -\frac{1}{2}\left(\frac{p+2}{p+1}\right)(n_{\rm s} - 1)^2. \tag{66}$$

This parameter will be very useful for higher orders and more accurate constraints in future observations. For instance, if it is considered the particular case with $p = 2$ and $n_{\rm s} = 1.2$, the running obtained is $dn_{\rm s}/d\ln k = -0.05$ (Kinney & Riotto 1998).

5.5. *Linear models:* $\eta = -\epsilon$

Linear models, $V(\phi) \propto \phi$, are located on the limit between large field and small field models. They are represented by $V''(\phi) = 0$ and $\eta = -\epsilon$. The spectral index and tensor-to-scalar ratio are given by

$$n_{\rm s} - 1 = -\frac{6}{4N+1}, \qquad r = \frac{4\pi}{4N+1}. \tag{67}$$

5.6. *Other models*

There still remain several single-field models which cannot fit into this classification, for instance the logarithmic potentials (Barrow & Parsons 1995)

$$V(\phi) = V_0 \left[1 + (Cg^2/8\pi^2) \ln(\phi/\mu)\right]. \tag{68}$$

Typically they correspond to loop corrections in a supersymmetric theory, where C denotes the degrees of freedom coupled to the inflaton and g is a coupling constant. For this potential, the inflationary parameters are

$$\begin{aligned} n_{\rm s} - 1 &\simeq -\frac{1}{N}\left(1 + \frac{3Cg^2}{16\pi^2}\right), \\ r &\simeq \frac{1}{N}\frac{Cg^2}{4\pi}. \end{aligned} \tag{69}$$

In this model, to end up inflation, an auxiliary field is needed, which is the main feature of hybrid models. However when it is plotted on the $n_{\rm s}$—r plane, is located into the small-field region.

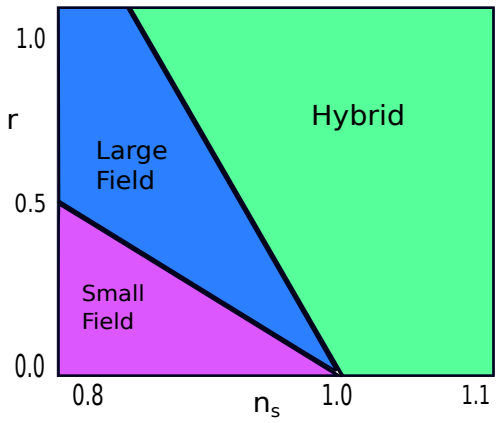

Fig. 7. Classification of the potentials in terms of $n_{\rm s}$ and r parameters.

The classification of inflationary models mentioned previously may be interpreted as an arbitrary one. Although, it is very useful because different types of models cover different regions of the $(n_{\rm s}, r)$ plane without overlaping, see Figure 7.

6. TESTING INFLATIONARY MODELS

How can observations constrain $n_{\rm s}$ and r in inflationary models? During several years many projects at different scales of the Universe, have been carried out in order to look for observational data to constrain cosmological models. Among many others, they are: Cosmic Background Explorer (COBE), Wilkinson Microwave Anisotropy Probe (WMAP), Cosmic Background Imager observations (CBI), Ballon Observations of Millimetric Extra-galactic Radiation and Geophysics (BOOMERang), the Luminous Red Galaxy (LRG) subset DR7 of the Sloan Digital Sky Survey (SDSS), Baryon Acoustic Oscillations (BAO), Supernovae (SNe) data, Hubble Space Telescope (HST) and currently the South Pole Telescope (SPT) and the Atacama Cosmology Telescope (ACT). Below, we show some predictions coming from different types of inflationary potentials, comparing them with current observational parameters (Mortonson et al. 2011). We mention some results that have been obtained on the phase space $n_{\rm s} - r$. At this stage, our interest is mainly focussed on the case with no running $dn_{\rm s}/d\ln k = 0$.

Figure 8 displays marginalised posterior distributions for $n_{\rm s}$ and r based on two different types of data sets: WMAP3 by itself, and WMAP3 plus information from the LRG subset from SDSS. Considering WMAP3 observations alone (Kinney et al. 2006), the parameters are constrained such that $0.94 < n_{\rm s} < 1.04$ and $r < 0.60$ (95% CL). Those models which present $n_{\rm s} < 0.9$ are therefore ruled out at high confidence level. The same is applied for models with $n_{\rm s} > 1.05$. WMAP data by itself cannot lead to a strong constraints because the existence of parameter degeneracies, like the well known geometrical degeneracy involving Ω_m, Ω_Λ and Ω_k. However, when it is combined with different types of experiments, together they increase the constraining power and might remove degeneracies. Furthermore, when the SDSS data are included the limit of the gravitational wave amplitude is reduced, whereas the spectral index parameter does not present any relevant change. For WMAP3+SDSS the constraints imposed on $n_{\rm s}$ and r are $0.93 < n_{\rm s} < 1.01$ and $r < 0.31$ (Kinney et al. 2006).

On the other hand, Figure 9 shows that with WMAP5 data alone, $r < 0.43$ (95% CL) while $0.964 < n_{\rm s} < 1.008$. When BAO and SN data are added, the limit improves significantly to $r < 0.22$ (95% CL) and $0.953 < n_{\rm s} < 0.983$. (Komatsu 2009).

Following the same line for inflationary models, we employ the COSMOMC package (Lewis & Bridle 2002) which allows us to produce some predictions for the $n_{\rm s}$ and r parameters given a dataset. To illustrate our point, we consider WMAP seven year data. We observe from Figure 10, that in order a model to be considered as a favourable candidate it has to predict a small field with spectral index about $n_{\rm s} = 0.982^{+0.020}_{-0.019}$ and a tensor-to-scalar ratio of $r < 0.37$ (95% CL). When WMAP-7 is combined with different datasets, the constraints are tighten as is shown by (Larson et al. 2011).

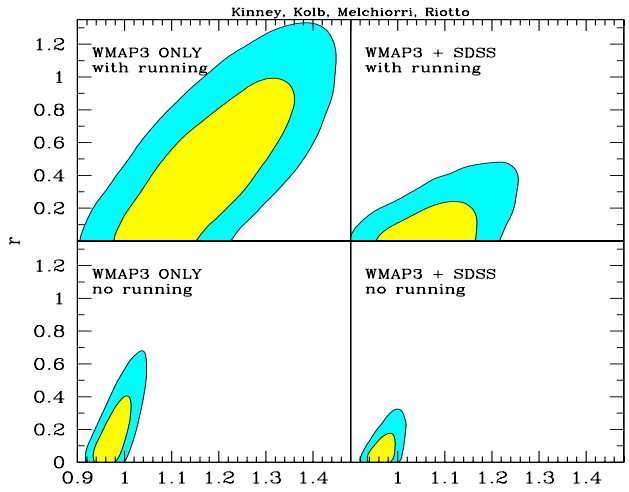

Fig. 8. WMAP3 data sets constraining $n_{\rm s}$ and r parameters. Coloured regions correspond to 68% and 95% CL (Kinney et al. 2006).

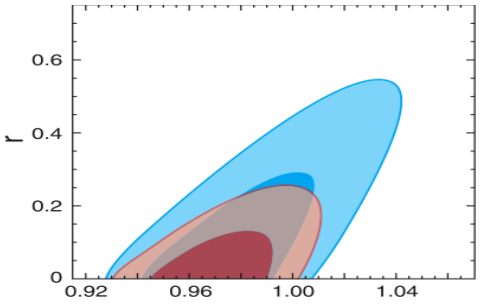

Fig. 9. Constraints on $n_{\rm s}$ and r. WMAP5 results are coloured blue and WMAP5+BAO+SN red, both on 68% and 95% CL (Komatsu 2009).

Future observations will reach higher accuracy and therefore strengthen the constraints. We build a simple toy model from an optimistic Planck-like sensitivity (Planck Collaboration 2006) using the best-fit parameters extracted from WMAP7 year as a fiducial values (see Figure 11). The constraints on $n_{\rm s}$ are highly improved using this idealised experiment: $n_{\rm s} = 0.968 \pm 0.006$ and $r < 0.15$ with 95% CL.

7. CONSTRAINTS ON INFLATIONARY MODELS

WMAP3 results are shown in Figure 12. Models with $n_{\rm s} = 1$ are in a good agreement with CMB data. In particular the Harrison-Zel'dovich model: $n_{\rm s} = 1, r = 0, dn_{\rm s}/d\ln k = 0$, is not ruled out at more than 95% CL from CMB data alone. Similarly, for inflation driven by a massless self-interacting scalar

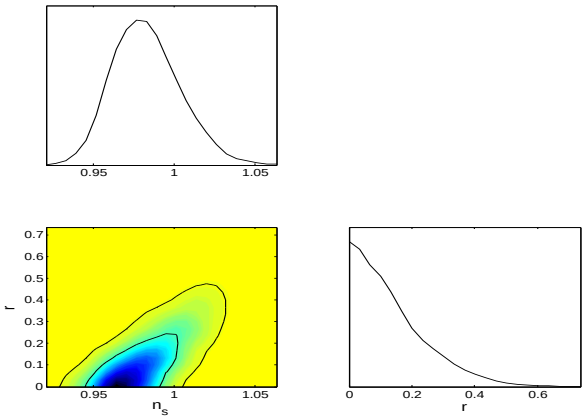

Fig. 10. Marginalised probability constraints on n_s and r using only WMAP7 data. 2D constraints are plotted with 1σ and 2σ confidence contours

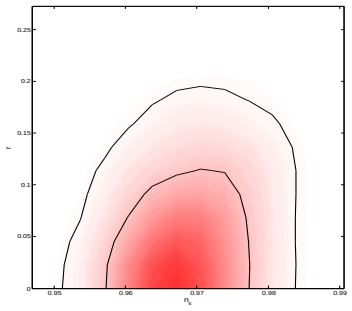

Fig. 11. 2D marginalised probability onstraints on n_s and r for a particular realisation at Planck-like sensitivity. 2D constraints are plotted with 1σ adn 2σ confidence contours.

field $V(\phi) = \lambda\phi^4$, the contours indicate that this potential with 60 e-folds is still consistent with the WMAP3 data at 95% CL.

On the other hand, WMAP5 results are summarised in Figure 13: The model $V(\phi) = \lambda\phi^4$, unlike WMAP3 constraints, is found to be located far away from the 95% CL, and therefore it is definitely excluded. For inflation produced by a massive scalar field $V(\phi) = (1/2)m^2\phi^2$, the model with $N = 50$ is situated outside the 68% CL, whereas with $N = 60$ is at the boundary of the 68% CL. Therefore, this model for the corresponding number of e-folds is consistent with data within the 95% CL. The points represented by N-flation describe a model with many massive axion fields (Liddle 1998). For an exponential potential, it is observed that models with $p < 60$ are mainly excluded.

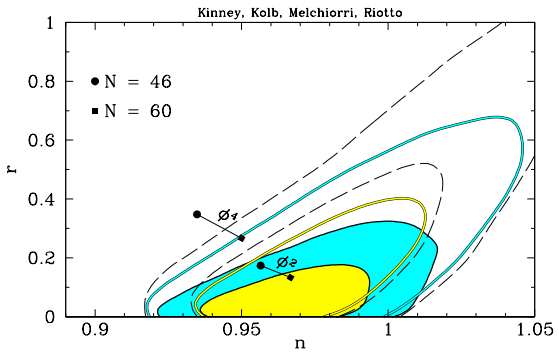

Fig. 12. WMAP3 (open contours) and WMAP3+SDSS (filled contours) constraints on phase space n_s, r. Contours with 68% CL and 95% are shown with dashed lines (Kinney et al. 2006).

Models with $60 < p < 70$ are roughly in the boundary of the 95% region, and $p > 70$ are in agreement within the 95% CL. Some models with $p \sim 120$ can be located in or outside the 68% CL, essentially they lay out in the limit.

The hybrid potentials, as was already noted, can have different behaviours depending on the (ϕ/μ) value. The parameter space can be split into three different regions based on (ϕ/μ). For $\phi/\mu \ll 1$ the dynamics is similar to small fields and the dominant term lays in the region called "Flat Potential Regime". For $\phi/\mu \gg 1$ the result is similar to large field models, this region is called "Chaotic Inflation-like Regime". The boundary, $\phi/\mu \sim 1$ is named "Transition regime". The different (ϕ/μ) values corresponding to their regions are shown in Figure 13.

Two recent experiments have placed new constraints on the cosmological parameters: the Atacama Cosmology Telescope (ACT; Dunkley et al. (2010)) and the South Pole Telescope (SPT; Keisler et al. (2011)). Figure 14 shows the predicted values for a chaotic inflationary model with inflaton potential $V(\phi) \propto \phi^p$ with 60 e-folds. We observe that models with $p \geq 3$ are disfavored at more than 95% CL.

8. CONCLUSIONS

Considering the analysis presented here is complicated to prove that a given model is correct, since these could be just particular cases of more general models with several parameters involved. However, it is possible to eliminate models or at least give some constraints on their behaviour leading to a narrower range of study.

Although we have presented some simple examples of potentials, the classification in small-field, large-field, and hybrid models is enough to cover the

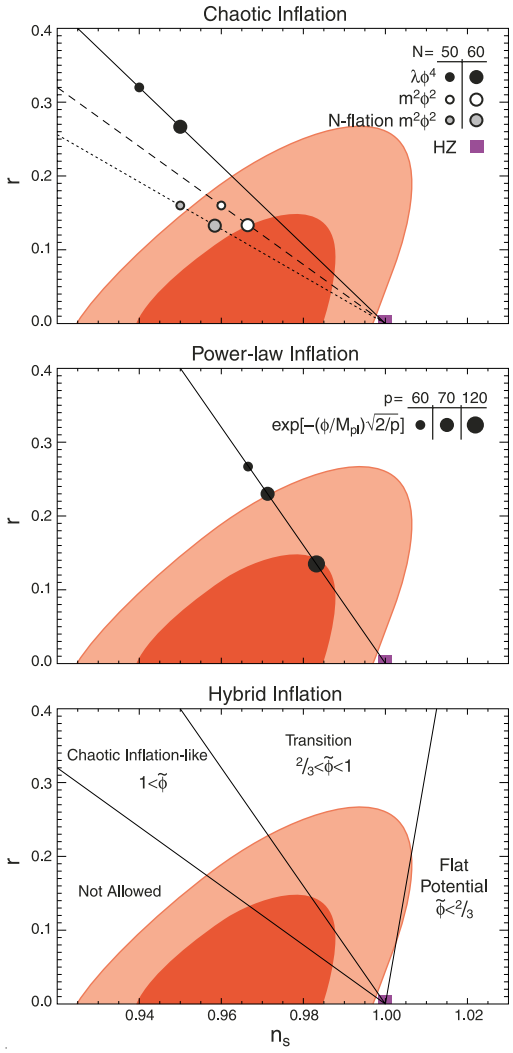

Fig. 13. Constraints on large and hybrid models obtained from WMAP5+BAO+SN. They are shown in contours with 68% and 95% CL (Komatsu 2009).

entire region of the $n_{\rm s}$–r plane as illustrated in Figure 7. Different versions of the three types of models predict qualitatively different scalar and tensor spectra, so it should be particularly easy to work on them apart.

We have seen that, the favoured models are those with small r (for $dn_{\rm s}/d\ln k \sim 0$) and slightly *red* spectrum, hence models with *blue* power spectrum $n_s > 1.001$ are inconsistent with the recently data. This simple but important constraint allows us to rule out the simplest models corresponding to hybrid inflation of the form $V(\phi) = \Lambda^4(1 + (\mu/\phi)^p)$. There still remain models with red spectra in the hybrid classification: inverted models and models with logarithmic potentials.

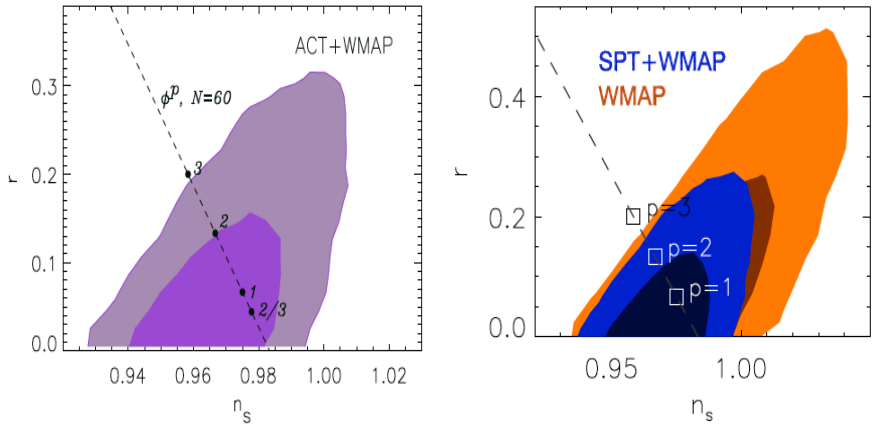

Fig. 14. Marginalized 2D probability distribution (68% and 95% CL) for the tensor-to-scalar ratio r, and the scalar spectral index n_s for ACT+WMAP (left panel) and SPT+WMAP (right panel) (Dunkley et al. 2010; Keisler et al. 2011).

Scale-invariant power spectrum $n_s = 1$ is consistent within 95% CL with WMAP3 data alone, considering no running of the spectral index. The HZ spectrum is therefore not ruled out by WMAP3. However, considering WMAP5 data, Figure 13 shows that HZ spectrum lays outside the 95% CL region, which indicates it is excluded considering the lowest order on the n_s, r parameters. When WMAP7 data without tensors is considered, scale-invariant spectrum is totally excluded by more than 3σ, however the inclusion of extra parameters weaken the constraint on the spectral index, in which case certain models are still consistent with HZ even for current observations. When chaotic models $V(\phi) \propto \phi^p$ are analysed with current data, it is found that quartic models ($p = 4$) are ruled out, whilst models with $p \geq 3$ are disfavoured at $> 95\%$ CL. Moreover, the quadratic potential $V(\phi) = 1/2m^2\phi^2$ is in agreement with all data sets presented here and therefore remains as a good candidate. Table 1 summarises the constraints on the n_s and r parameters and its improvements through the years. Future surveys will provide a more accurate description of the universe and therefore narrow the number of candidates which might better explain the Inflationary period.

9. ACKNOWLEDGMENTS

JAV was supported by CONACyT México.

REFERENCES

Albrecht, A., and Steinhardt, P. J. 1982, Phys. Rev. Lett., 48, 1220
Ambrosio, M., et al. 2002, Eur. Phyis. J. C., 25, 511
Barrow, J. D., and Parsons, P. 1995, Phys. Rev. D, 52, 10

TABLE 1

SUMMARISE OF THE $n_{\rm s}$, r CONSTRAINTS FROM DIFFERENT MEASUREMENTS [a].

Parameter	Limits	Data set
$n_{\rm s}$	0.968 ± 0.006	PLANCK (idealised)
r	< 0.15	
$n_{\rm s}$	0.9711 ± 0.0099	SPT+WMAP7+BAO+H_0
r	< 0.17	
$n_{\rm s}$	0.970 ± 0.012	ACT+WMAP7+BAO+H_0
r	< 0.19	
$n_{\rm s}$	0.973 ± 0.014	WMAP7 + BAO +H_0
r	< 0.24	
$n_{\rm s}$	$0.982\pm^{+0.020}_{-0.019}$	WMAP7 ONLY
r	< 0.36	
$n_{\rm s}$	0.968 ± 0.015	WMAP5+BAO+SN
r	< 0.22	
$n_{\rm s}$	0.986 ± 0.022	WMAP5 ONLY
r	< 0.43	
$n_{\rm s}$	0.97 ± 0.04	WMAP3 + SDSS
r	< 0.31	
$n_{\rm s}$	0.99 ± 0.05	WMAP3 ONLY
r	< 0.60	

[a]Peiris et al.2003; Kinney et al.2006; Komatsu et al.2009; Komatsu et al.2011; Dunkley et al. 2010; Keisler et al. 2011

Barrow, J. D., Tipler, F. J., 1986, The Anthropic Cosmological Principle, Clarendon Press, Oxford, UK
Baumann, D., and Peiris, H. V. 2009, Adv. Sci. Lett., 2, 105
Carroll, S. 2001, Living Rev. Relativity, 3
Coles, P., and Lucchin, F. 1995, Cosmology, WILEY, England, UK
Copeland, E. J., et al. 1994, Phys. Rev. D, 49, 6410
Dodelson, S. 2003, Modern Cosmology, Academic Press, Amsterdam, Netherlands
Dunkley, J., et al. 2010, astro-ph/1009.0866.
Georgi, H., Glashow, S. L. 1974, Phys. Rev. Lett., 32, 438
Gold, B., et al. 2011, ApJS, 192, 15
Guth, A. H. 1997, The Inflationary Universe, Ed. Vintage
Guth, A. H. 1981, Phys. Rev. D, 23, 347
Hu, W., and Dodelson, S. 2002, Annu. Rev. Astron. and Astrophys., 40, 171
Hinshaw, G., et al. 2009, ApJS, 180, 225
Keisler, R., et al. 2011, astro-ph/1105.3182
Kinney, W . H. 2004, CU-TP-1083, astro-ph/0301448
Kinney, W. H., et al. 2006, Phys. Rev. D, 74, 023502

Kinney, W. H., and Riotto, A., 1998, Phys. Lett., 435B, 272
Kolb, E. W., Turner, M. S. 1983, Ann Rev Nucl Part Sci. 33, 645
Kolb, E. W., Turner, M.S. 1994, The Early Universe, Westview Press
Komatsu, E., et al. 2009, ApJS., 180, 330
Komatsu, E., et al. 2011, Astrophys. J. Suppl., 192, 18
La, D., and Steinhardt, P.J. 1999, Phys. Rev. D, 59, 064029
Larson, D., et al. 2011, ApJS., 192, 16
Lewis A., and Bridle, S., 2002, Phys. Rev D, 66, 103511
Liddle, A. 1999, AIP Conf. Proc., 476, 11
Liddle, A., Mazundar, A., and Schunck, F. E. 1998, Phys. Rev. D, 58, 061301
Liddle, A. 1999, An introduction to Modern Cosmology, WILEY, England, UK
Liddle, A. R., and Lyth, D. H. 2000, Cosmological inflation and large-scale structure, Cambridge University Press, Cambridge, UK
Liddle, A.R. and Lyth, D.H 1992, Phys. Lett. B, 291, 39
Liddle, A. R., et al. 1994, Phys. Rev. D, 50, 12
Linde, A. D. 1982, Phys. Lett. B, 108, 389
Linde, A. D. 1983, Phys. Lett. B, 129, 177
Linde, A. D. 1990, Particle Physics and Inflationary Cosmology, Harwood Academic, Switzerland
Linde, A. D. 1991, Phys. Lett. B, 259, 38
Linde, A. 2005, J.Phys.Conf.Ser., 24
Lidsey, J. E., et al. 1997, Annu. Rev.Mod.Phys., 69, 373
Lyth, D. H., and Riotto, A. 1999, Physics Reports, 314, 1
Mortonson, M. J., Peiris, H.V., and Easther, R. 2011, Phys.Rev. D, 83, 043505
Mukhanov, V. F., and Chibisov, G. V. 1997, JETP Letters, 33, 532
Olive, K. A. 1990, Physics Reports, 190, 307
Peiris, H. V., et al. 2003, ApJS., 148, 213
The Planck Collaboration, 2006, astro-ph/0604069.
Riess, A. G., et al. 2009, ApJ., 699, 539
Smooth, G. F., et al. 1992, ApJ Letters, 396, L1
Springel, V., et al. 2005, Nature, 435, 629
Tegmark, M., et al. 2001, Phys. Rev. D, 63, 043007
Vilenkin, A., Shellard, E. P. S. 2000, Cosmic Strings and Other Topological Defects, Cambridge University Press, Cambridge, UK

J. Alberto Vázquez: Kavli Institute for Cosmology, Madingley Road, Cambridge CB3 0HA, UK.
Astrophysics Group, Cavendish Laboratory, JJ Thomson Avenue, Cambridge CB3 0HE, UK. (jv292@cam.ac.uk)